All-in-one Image Restoration for Unknown Degradations Using Adaptive Discriminative Filters for Specific Degradations

Dongwon Park[1,4], Byung Hyun Lee[2], Se Young Chun[1,2,3,†]
[1]INMC, [2]Dept. of ECE, [3]IPAI, Seoul National University, Republic of Korea
[4]Dept. of EE, UNIST, Republic of Korea
{dong1park,ldlqudgus756,sychun}@snu.ac.kr

Abstract

Image restorations for single degradations have been widely studied, demonstrating excellent performance for each degradation, but can not reflect unpredictable realistic environments with unknown multiple degradations, which may change over time. To mitigate this issue, image restorations for known and unknown multiple degradations have recently been investigated, showing promising results, but require large networks or have sub-optimal architectures for potential interference among different degradations. Here, inspired by the filter attribution integrated gradients (FAIG), we propose an adaptive discriminative filter-based model for specific degradations (ADMS) to restore images with unknown degradations. Our method allows the network to contain degradation-dedicated filters only for about 3% of all network parameters per each degradation and to apply them adaptively via degradation classification (DC) to explicitly disentangle the network for multiple degradations. Our proposed method has demonstrated its effectiveness in comparison studies and achieved state-of-the-art performance in all-in-one image restoration benchmark datasets of both Rain-Noise-Blur and Rain-Snow-Haze.

1. Introduction

Image restoration is a fundamental computer vision task that has been widely investigated especially for single degradation such as noise, blur, snow or rain in images. Recently, deep learning-based approaches have demonstrated remarkable performance with fast computations, but a majority of them have been focusing on known single degradation such as denoising [2, 4, 20, 25, 65, 67, 68], deraining [5, 16, 30, 51, 52, 59, 60], deblurring [19, 23, 24, 36, 38, 43, 46, 55], desnowing [11, 31, 33, 53] and dehazing [9, 18, 27, 32, 40, 45, 56, 63, 66]. These prior works can enhance the visual quality of deteriorated images as well as may improve the performance of down-stream tasks including classification [17, 22], object detection [41, 42] and autonomous driving [3, 34]. However, they are limited only to known single degradation cases, thus can not reflect unpredictable realistic environments with unknown multiple degradations, which may change over time.

Image restoration for real-world environments is a challenging problem since it must deal with unknown multiple degradations. Since most prior works for single degradation may not be optimal for multiple degradations, image restorations for known and unknown multiple degradations have recently been investigated, showing promising results, but require large networks and/or heavy computations. One approach to handle known multiple degradations is to develop a single network architecture and train it with different degradation datasets to generate independent models (IMs) for various degradations as illustrated in Figure 1(a). This approach has achieved state-of-the-art performance for known multiple degradations [7, 8, 13, 35, 39, 50, 54, 61, 62]. However, it requires a trained independent network for each degradation task and a proper IM should be selected to handle incoming images with known multiple degradations. Thus, this approach can be applied only to the case of known multiple degradations and it still can not reflect realistic environments with unknown degradations.

Recently, all-in-one image restoration for unknown multiple degradations has been proposed [12, 26, 29] with different approaches. The first way to handle unknown multiple degradations is to use a shared decoder with multiple independent encoders for multiple degradations (will denote it as Model with independent Encoders or ME) [29] to take the advantage of using small network parameters as compared to IM as illustrated in Figure 1(b). However, this architecture requires more independent encoders to handle more degradations inefficiently while there may be interference among diverse degradations in the shared decoder. The second way is to use a unified model (UM) with a pair of shared encoder and decoder for multiple degradations [12]

†Corresponding author.

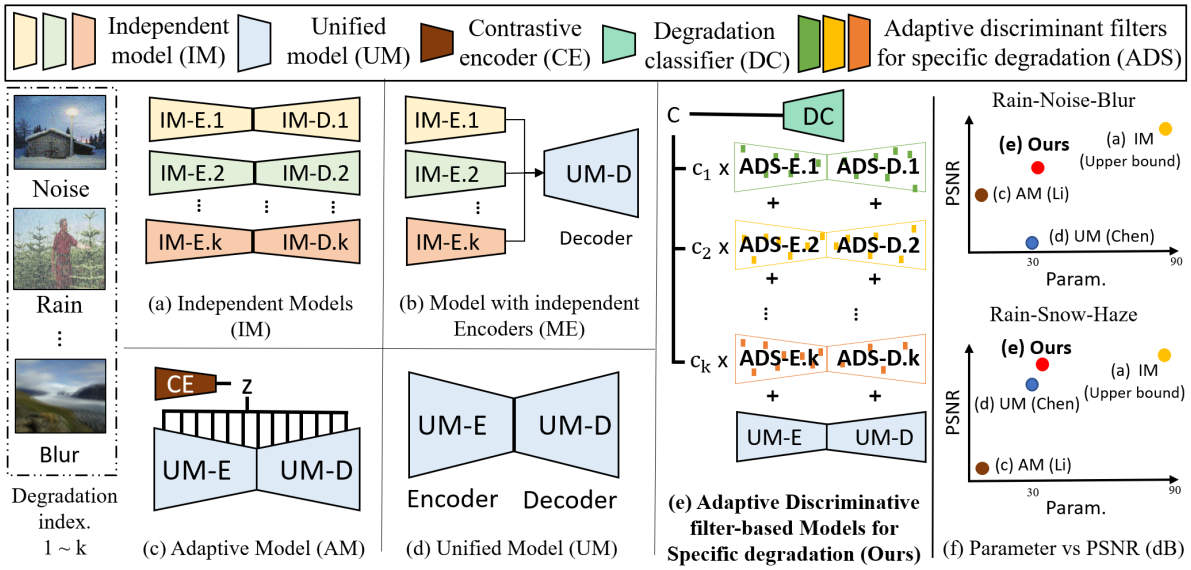

Figure 1. Illustrations of 5 image restoration methods for multiple degradations. (a) Independent models (IM) where the models IM.1, IM.2 and IM.k are independent, (b) Model with independent Encoders (ME) whose encoders IM.1, IM.2 and IM.k are independent, (c) Adaptive Model (AM), (d) Unified Model (UM) and (e) our proposed Adaptive Discriminant filter-based Model for Specific degradation (ADMS) where the sparse models ADS.1, ADS.2 and ADS.k are independent. (f) Number of parameters (Million) vs. PSNR (dB). Our proposed method (Ours) outperformed state-of-the-art all-in-one image restoration methods on both Rain-Noise-Blur and Rain-Snow-Hazy datasets.

as illustrated in Figure 1(d). Training was done with knowledge distillation for multiple degradations. However, this UM may not be ideal considering different restoration characteristics in processing multiple degradation tasks. For example, noise removal is mainly low-pass filtering, but deblurring is close to high-pass filtering. The third way to restore unknown multiple degradations is to use the same UM, but with an adaptive model (AM) using a contrastive degradation module (Contrastive Encoder or CE) [26] as illustrated in Figure 1(c). This CE was trained implicitly to represent multiple degradations so that UM can perform the restoration process given the corresponding degradation information. However, this architecture is still using the same unified model, which may not be the best for multiple restoration tasks in a single model.

In this work, we propose an all-in-one image restoration method for unknown multiple degradations by taking the advantages of both high-performing IMs and memory-efficient UMs. We designed our network to use a small number of independent parameters (usually 1-5%) for each degradation task additionally so that network parameters are partially, but explicitly disentangled for different tasks without increasing memory usage much as illustrated in Figure 1(e). Additional sparse parameters can be located and used adaptively by leveraging the Filter Attribution method based on Integral Gradient (FAIG) [57], which was originally used to find the most discriminative filters for degradation removal in super-resolution networks. A degradation classifier (DC) for multiple degradations is designed to adaptively select the degradation type for incoming images so that appropriate Adaptive Discriminant filters for Specific degradations (ADS) can be used for inference. We call the proposed method Adaptive Discriminant filter-based Models for Specific degradation (ADMS) using ADS and DC modules depicted in Figure 1(e).

We summarize four contributions of this work: (1) We propose an ADMS with "explicitly" separated, sparsely added discriminative network parameters (3%) for different degradations to ensure partial independence between different tasks. (2) By extending the FAIG [57] to diverse degradation cases, we leverage it to locate discriminative network parameters (3%) for specific degradation.(3) We propose the DC that leverages our ADS for handling unknown multiple degradations. (4) Our proposed ADMS achieved state-of-the-art performance for diverse combinations of multiple degradations such as Rain-Noise-Blur and Rain-Snow-Haze, as shown in the Figure 1(f).

2. Related work

2.1. Physical models for single degradation

To understand different types of multiple degradations, we review the physical models for single degradation such as noise, cloudiness, snow and rain. The noise image is typically represented by the following physical model:

$$x_{\text{noise}} = x^{\text{gt}} + \epsilon, \quad \epsilon \sim \mathcal{N}(0, \sigma_\epsilon^2 I) \tag{1}$$

where x_{noise}, x^{gt}, ϵ and σ_ϵ^2 denote a noisy image, a clean image, a noise vector and variance, respectively. Typically, a denoising function exhibits the characteristics of low-pass filters to reduce high frequency information of noise.

The blurring processing is generally represented with the following physical corruption model:

$$x_{\text{blur}} = x^{\text{gt}} * B \tag{2}$$

where x_{blur}, B and $*$ denote a blur image, a blur kernel and a convolution, respectively. A typical deblurring function has the characteristics of a high-pass filter to recover high frequency details. Thus, the restoration process for noise and blur seems to have quite different characteristics.

Raining, snowing and hazing is represented with the following physical corruption model [1, 10, 11, 37, 49, 58]:

$$x_{\text{rain,snow,haze}} = T \odot (x^{\text{gt}} + S) + (1 - T) \odot A \tag{3}$$

where $x_{\text{rain,snow,haze}}$ denotes a rain, snow or haze degraded image. $\odot$, 1, A, T, S are element-wise multiplication, matrix of ones, atmospheric light, medium transmission map, rain or snow streak. Note that the physical corruption models of raining, snowing and hazing degradations have similar structures and characteristics.

2.2. Restoration for known multiple degradations

Although IM achieves state-of-the-art performance for single degradation, it requires multiple networks to cover all necessary degradations. Recently, MPRNet was proposed based on multi-stage architecture to progressively learn the image restoration functions for known multiple degradations [62]. Deep Generalized Unfolding Network (DGUNet) was proposed based on Proximal Gradient Descent (PGD) algorithm for a gradient estimation strategy without loss of interpretability [35]. A vision transformer-based Image Processing Transformer (IPT) was proposed in [6] and Restormer, an efficient transformer model that can be applied to large images while capturing long-range pixel interactions using a multi-head attention and feed-forward network, was also proposed in [61]. A Swin-transformer-based Uformer block was proposed that enhances local attention instead of global self-attention [54]. A multi-axis gated MLP-based MAXIM method was proposed that allows efficient and scalable spatial mixing of local and global information [50]. SPAIR, a network design that dynamically adjusts calculations for difficult areas of an image, was proposed in [39] and an efficient and simple model without nonlinear functions was proposed in [7]. Class-SR [21] proposed an SR inference using different networks for each patch, similar to the IM technique.

2.3. All-in-one image restoration

Li *et al.* [29] proposed a neural architecture search for all-in-one image restoration focusing on Rain-Haze-Snow dataset using task-specific encoders Chen *et al.* [12] proposed a two-stage knowledge learning mechanism based on multi-teacher and single-student approach for multiple degradations, also focusing on Rain-Haze-Snow dataset. However, this work was effective only for similar degradations like Rain-Haze-Snow (see (3)) and not for different degradations such as Rain-Noise-Blur (see (1), (2) and (3)), as illustrated in Figure 1(f). Li *et al.* [26] proposed a Contrastive based degraded Encoder (CE) and degradation-guided restoration network that adaptively improves performance in various degradations, including Rain-Noise-Blur. However, it did not not perform well in different degradations like Rain-Haze-Snow, as shown in Figure1(f).

Our proposed ADMS approach for all-in-one image restoration is unique as it ensures partial independence among tasks using sparsely added discriminative network parameters for specific degradations and adaptive efficiency by selecting task-specific partial parameters with a degradation classifier.

3. Discriminative Filters for Degradations

3.1. Problem formulation

UM restores unknown degraded images via noise, blur, rain, snow and/or haze to clean images by minimizing the following loss function :

$$\mathcal{L}(\theta_{um}) = \sum_{d=1}^{k} \sum_{n=1}^{N_d} \left\| G(x_{n,d}; \theta_{um}) - x_{n,d}^{\text{gt}} \right\| \tag{4}$$

where d denotes an index for specific degradation types such as noise, rain, and blur, N_d is the number of training samples for a specific task d, G and θ_{um} denote the network structure and its network parameters of UM, $\|\cdot\|$ represents the l_1 norm and $x_{n,d}$ is a degraded image for the degradation d with its corresponding ground truth $x_{n,d}^{\text{gt}}$.

IMs are multiple networks with the same structure and independent network parameters for each degradation. For k different degradations, IMs require k times larger models than UM, where the network parameters for each degradation are defined as $\{\theta_d\}_{d=1}^{k}$. A proper IM must be selected for an incoming degraded image by predicting the type of degradation. While IMs achieve high performance with the specialized model for each task, they require much larger number of network parameters.

3.2. Filter attribution integrated gradients

Xie *et al.* [57] proposed FAIG that can identify discriminative filters of specific degradation in blind super-resolution (SR) by computing integrated gradient (IG) [47, 48] between the baseline and target models. The baseline model represents the "absence" of the desired function (*e.g.*, performing SR) defined as θ_{ab} and the target model

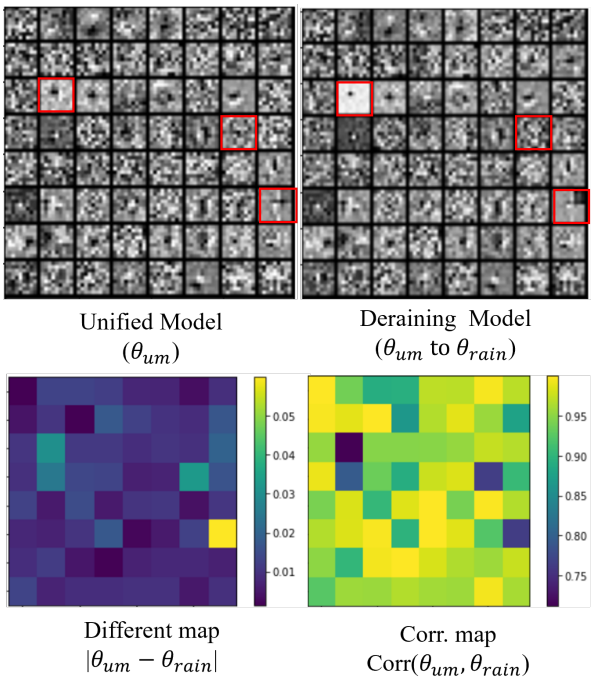

Figure 2. Visualization of convolution filters in UM for Rain-Noise-Blur and IM for Rain where IM was fine-tuned from UM along with the difference and correlation maps between them.

is defined as θ_{ta} for all desired tasks. Let us denote $\lambda(\alpha)$, $\alpha \in [0, 1]$ as a continuous path between the baseline and the target models such that $\lambda(1) = \theta_{ab}$ and $\lambda(0) = \theta_{ta}$. For a fixed input image x, this continuous path can simply be $\lambda(\alpha) = \alpha\theta_{ab} + (1 - \alpha)\theta_{ta}$. Then, the FAIG on the continuous path between two models is discretized as [57]:

$$\mathrm{F}_i(\theta_{ta}, \theta_{ab}, x) \approx \left| \frac{1}{N}[\theta_{ta} - \theta_{ab}]_i \sum_{t=0}^{N-1} \left[\frac{\partial \mathcal{L}(\lambda(\alpha_t), x)}{\partial \lambda(\alpha_t)} \right]_i \right| \tag{5}$$

where $\alpha_t = t/N$ with the number of points on the path for integral approximation N and the index of the network kernel i. The FAIG was evaluated for denoising, deblurring and SR [57]. We leverage the FAIG to investigate the properties of UM and IM for diverse multiple degradations.

3.3. Toy experiment for analyzing UM vs. IM

Inspired by [57], we performed a toy experiment consisting of a simple CNN structure of SRCNN [14] which was trained on Rain-Noise-Blur as a UM so that the network parameter θ_{um} was obtained and fine-tuned the pre-trained UM with θ_{um} on Rain only to obtain an IM with network parameter θ_{rain}. Then, we visualized the first layer filters of those two networks (θ_{um}, θ_{rain}) with normalization in the top of Figure 2 and presented difference/correlation maps between θ_{um} and θ_{rain} in the bottom of Figure 2.

We observed that a small number of kernels in θ_{rain} were updated from θ_{um} as marked with the red boxes in the top of Figure 2, but the rest of the filters maintained similar visual patterns. This observation is consistent with the results of [57] for different degradations. This toy experiment suggests that the findings in [57] can also be used for other degradations - there are the most discriminative filters for specific degradation removal. UM has no guarantee to preserve these discriminative filters when trained for multiple degradations. However, our proposed method will ensure the preservation of these discriminative filters for specific degradations by explicitly disentangling them.

4. Proposed All-in-one Image Restoration

Figure 3 shows ADMS which contains unknown multiple degradations with Degradation Classifier (DC) and Convolutional Neural Network (CNN) with Adaptive Discriminative filters for Specific degradation (ADS). The locations of ADS are selected by our FAIG for Specific Degradation.

4.1. FAIG for specific degradations

We leveraged the FAIG [57] in (5) to locate discriminative filters for specific degradation. The original FAIG can be computed by putting unified model for all desired task as the target and a model with the "absence" of the desired functions as baseline.Here we propose the FAIG with Specific Degradation (FAIG-SD) with IM for one degradation as the target and UM for all degradations as the baseline.

Specifically, the baseline model is the unified model θ_{um} trained for all degradations and the target model θ_d for the specific degradation d is constructed by fine-tuning the baseline model. For k degradations, there are k target models so that computing FAIG with (5) can yield $\mathrm{F}_i(\theta_d, \theta_{um}, x)$ for multiple degradations $d = 1, \ldots, k$ and all kernels i. Then, all FAIG scores are sorted in descending order and the kernels with the top $q\%$ scores are selected for each d where $q = 1 \sim 5$ is fixed. Selected kernel indices are used to generate masks (M_d) with 1 for selected kernels and 0 otherwise as illustrated in Figure 3(b).

4.2. Degradation classifier

The Degradation Classifier (DC) aims to classify the degradation type d from the input x_d. We propose a degradation classification network P to adaptively change the network parameters in the CNN with ADS. The degradation type of each input x_d is distinguished through $\hat{C} = P(x_d)$, which is an estimated degradation type or $\hat{C} = \{\hat{c}_d\}_{d=1}^{k}$. To enhance the estimation process efficiency, we design a lightweight network P that consists of 5 CNN layers, a global average layer and a fully connected layer. A cross entropy loss was used to optimize the network P. The presence of DC in ADMS leads to an improvement of 0.17dB on average in Rain-Blur-Noise.

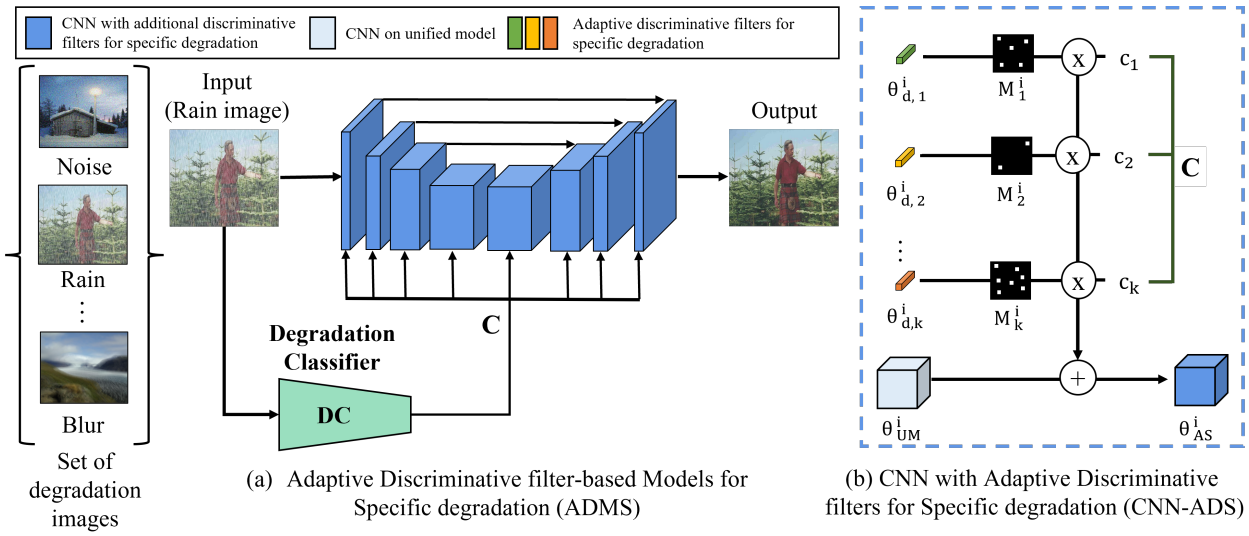

Figure 3. Our proposed method with (a) overall structure and (b) CNN with adaptive discriminative filters for specific degradation.

4.3. CNN with adaptive discriminative filters

We propose a CNN (UM) with ADS (Adaptive Discriminative filters for Specific degradation), implemented by the masks M_d that are constructed using our FAIG-SD and the predicted degradation probability $\hat{C}$ as illustrated in Figure 3(b). Specifically, M_d is a mask for filters in the network such that 1 is assigned only to the filter indices whose FAIG-SD values are the top $q\%$ scores for a degradation type d. $\hat{C}$ is the predicted degradation type where the sum of all $\hat{c}_d$ is 1 and each $\hat{c}_d$ is in between 0 and 1. Then, the adaptive network kernel θ_{as} of our proposed CNN with ADS is defined as follows:

$$\theta^i_{ads} = \theta^i_{um} + \sum_{d=1}^{k} \hat{c}_d \, \theta^i_d \odot M^i_d \tag{6}$$

where $\odot$ is point-wise multiplication, i is kernel index and θ^i_d is an additional kernel for specific degradation d. If M^i_d has 0, the kernel θ^i_d does not exist and only θ^i_{um} is used. If it has 1, it operates as an CNN with ADS.

We set the portion of 1 in the mask to 3% in general, but other portions such as 1% or 5% were also investigated. For example, the mask active portion is 3% for 3 degradation types, our proposed method uses additional 9% of the entire network parameters as compared to the UM.

For training, we first train a UM (θ_{um}) for all degradation tasks. Then, we extract discriminative filter indices to form the masks M_d using our FAIG-SD for each degradation. Lastly, retraining is performed using our CNN with ADS. During retraining, only additional parameters θ_d are updated while the pre-trained UM is fixed. Our method proposes an efficient method in various degradation tasks by replacing only the important kernels for each task with the adaptive CNN kernels in the UM.

5. Experiments

We evaluated the proposed ADMS with Rain-Blur-Noise and Rain-Snow-Hazy datasets. For Rain-Noise-Blur, denoising has a low-pass filter tendency, while deblurring has a high-pass filter tendency. Thus, this dataset seems to contain different degradations corresponding to the models in (1), (2) and (3) and contradictory operations may be embedded in the same network. For Rain-Snow-Hazy, multiple degradations seem to share similar corruption model as in (3), thus similar operations may have synergetic effects for similar degradations [12]. We adopt an architecture similar to MSBDN [15], just like Chen [12] and NAFNet [7]. We used the official codes of Airnet [26] and Chen [12]. Details of the experimental environment are in the supplement.

Rain-Noise-Blur dataset: We evaluated our proposed method with the DID-dataset [64]. We trained on a DID train dataset of 5,000 images and tested on a DID test dataset of 1,200 images. In the case of rain, we used different levels of rain, as originally included in the DID training data and testing. In the case of noise, we produced a representative Gaussian noise image [25, 67, 68], and standard deviation was in between 20 and 50. In the case of blur, a blur image was generated using a centered blur kernel [43, 44], and the kernel size was in between 5 and 29.

Rain-Hazy-Snow dataset: We evaluated our proposed method with the Rain ("Rain 1400" [16]), Snow ("CSD" [11]) and Haze ("RESIDE" [28]) datasets similar to Chen *et al.* [12]. Rain 1400 contains 12600 composite images. CSD contains 10K mixed degradation of hazy and snow images. RESIDE consists of ITS , OTS and SOTS dataset. We trained on sample 5000 images from each dataset and used the Rain 1400 test data, CSD test data, and RESIDE SOTS dataset for testing.

Table 1. Performance comparisons among different filter location selections for M in our CNN with ADS: Random selection method (Ran), Encoder selection method (En), $|\theta - \hat{\theta}|$ selection method ($|\theta|$) and our FAIG-SD method (Ours) on Rain-Noise-Blur test dataset.

Added	Added 5% filters				Added 3% filters				Added 1% filters				Base
Task	Ran	En	$\|\theta\|$	**Ours**	Ran	En	$\|\theta\|$	**Ours**	Ran	En	$\|\theta\|$	**Ours**	UM
Rain	32.23	32.45	32.60	**32.80**	32.19	32.44	32.52	**32.74**	32.15	32.35	32.37	**32.56**	32.12
Noise	31.04	31.25	31.32	**31.46**	31.01	31.24	31.26	**31.42**	30.98	31.17	31.14	**31.30**	30.97
Blur	26.81	26.85	27.22	**27.70**	26.74	26.85	27.06	**27.57**	26.65	26.77	26.85	**27.28**	26.61
Avg.	30.03	30.18	30.38	**30.65**	29.98	30.17	30.28	**30.58**	29.93	30.10	30.12	**30.38**	29.90
Par.	33.0 M = 28.7M ×1.15				31.3 M = 28.7 M ×1.09				29.6 M = 28.7 M ×1.03				28.7

5.1. Comparison studies for different mask selection

We compared different mask (M) selection methods for our proposed CNN with ADS architecture in the Rain-Noise-Blur dataset to demonstrate the effectiveness of our FAIG-SD strategy.The selection ratios of the masks M were set up as 1%, 3% and 5%. The baseline network was the UM with MSBDN. Adaptive network kernels are added proportionately with the ratio of M. We investigated the following selection methods for the masks M: Random selection method (Ran), Encoder selection method only (En) following Li [29], $|\theta - \hat{\theta}|$ selection method (θ), and the proposed FAIG-SD method (described in Section 4.1 (Ours)).

The results are summarized in Table 1. Our method yielded substantially higher performance than other methods, demonstrating the effectiveness of selecting discriminative filters for each task. The discriminative filters seem to be specialized filters for each task.

5.2. Comparisons among all-in-one methods

Evaluations on Rain-Noise-Blur: We evaluated our ADMS for MSBDN (MSB) and NAFNet (NAF) networks on Rain-Noise-Blur dataset. Table 2 summarizes the performance in PSNR (dB) and the number of parameters. The IM method requires three times as many network parameters as the UM method with explicitly separated structure for multiple degradations, so it can be viewed as an upper-bound for performance. Our ADMS yielded significantly improved performance by 0.28 dB and 0.68 dB using slightly increased network parameters by 1.8 M (about 10.5%) and 2.9 M (about 10%) in NAF and MSB, respectively. Our proposed method with NAF achieved the performance very close to the upper bound by the IM with NAF (31.56 dB vs. 31.64 dB) and our proposed method with MSB yielded significantly higher performance then M-L (30.58 dB vs. 30.02 dB) with less number of parameters (31.6 M vs. 34.6 M). Note that MSBDN-Large (M-L) increases the network block in the MSBDN. These results demonstrated that our proposed method efficiently and effectively improved the performance in image restoration for multiple degradations.

Table 2. Quantitative performance comparison (Airnet [26] and Chen [12]) on the Rain-Blur-Noise test dataset in PSNR (dB), parameter size (Par in Million). Net is network architecture. MSBDN-Large (M-L) has increased network parameters by 5.9M. The inference speed of MSBDN (MSB) and NAFNet (NAF) were 0.3 seconds while AirNet took 0.9 seconds.

Net	M	Rain	Blur	Noise	Avg.	Par.
NAF	IM	33.03	30.30	31.59	31.64	**51.3**
MSB	IM	33.02	28.79	31.52	31.11	**83.1**
NAF	UM	32.99	29.46	31.39	31.28	17.1
MSB	UM	32.12	26.61	30.97	29.90	28.7
M-L	UM	32.25	26.81	31.00	30.02	34.6
MSB-Chen		32.14	25.91	30.85	29.63	28.7
Airnet		32.49	26.84	31.41	30.25	7.6
NAF	**Ours**	**33.15**	**29.99**	**31.53**	**31.56**	18.9
MSB	**Ours**	**32.74**	**27.56**	**31.42**	**30.58**	31.6

We also compare our ADMS with the existing methods such as Chen [12] and Airnet [26]. In Table 2, Chen [12] was originally developed for Rain-Snow-Haze, but in this work, we evaluated it on Rain-Blur-Noise dataset, which has a different combination of degradations. In this case, Chen [12] yielded similar or lower results than a simple UM. It seems that knowledge distillation is less effective for multiple teachers with different characteristics. However, thanks to the ADMS, our proposed method yields the highest PSNR among all-in-one methods [12, 26] by additionally using small network parameters compared to existing methods based on NAFNet and MSDBN networks.

Evaluations on Rain-Snow-Hazy: We evaluated our proposed ADMS on the Rain-Snow-Hazy benchmark dataset in Table 3. Chen [12] method yielded improved results compared to UM on this dataset with similar degradation. However, Airnet [26] that was developed for Rain-Blur-Noise yielded lower results in a combination of similar degradations. We analyzed this shortly. This table also showed that our proposed ADMS outperformed all prior arts for all-in-one image restoration methods. Furthermore, the modified version of Chen [12] with our proposed ADMS (Chen, Ours) yielded improved the performance by 0.64 dB compared to the original one. Figure 6 illustrates the results on Rain-Blur-Noise and Rain-Snow-Haze datasets visually. Our ADMS seems to yield better image restoration results than prior arts such as Chen [12] and AirNet [26].

Table 3. Quantitative performance comparison (Airnet [26] and Chen [12]) on the Rain-Snow-Hazy test dataset in PSNR (dB), parameter size (Param in Million). The inference speed of MSBDN (MSB) and NAFNet (NAF) is 0.3 seconds and AirNet is 0.9 seconds. "Chen, Ours" is a method to combine ours with Chen [12].

Net	M	Rain	Snow	Hazy	Avg.	Par.
MSB	IM	34.81	31.42	31.67	32.63	86.1
MSB	UM	30.77	30.56	30.45	30.59	28.7
MSB-Chen		31.52	32.28	30.54	31.45	28.7
Airnet		30.08	26.91	26.11	27.70	7.6
MSB	Ours	**32.07**	32.41	30.38	31.62	31.6
MSB	Chen, Ours	31.89	**33.83**	**30.56**	**32.09**	31.6

It is worth noting that our proposed ADMS outperformed other existing methods [12, 26] on both Rain-Blur-Noise and Rain-Snow-Haze datasets, which have different combinations of degradations. In contrast, the compared prior arts [12, 26] failed to achieve good performance on different dataset and seems to overfit to the respective dataset.

5.3. Empirical analysis on degradation classifier

Figure 4 illustrates the degradation representations of the CE in AirNet [26] and our proposed DC. Degradation representations for both Rain-Blur-Noise and Rain-Snow-Haze were generated and were visualized using t-SNE. We observed that AirNet [26] was unable to generate discriminant clusters in Rain-Snow-Haze that have similar degradation models. However, our DC generated discriminant

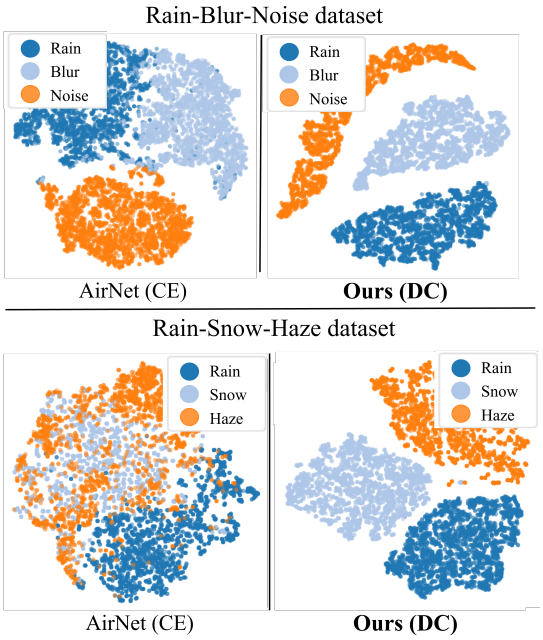

Figure 4. Visualization of representations for degradation types such as the similar combinations of degradation, Rain-Blur-Noise and different combination of degradation, Rain-Snow-Haze.

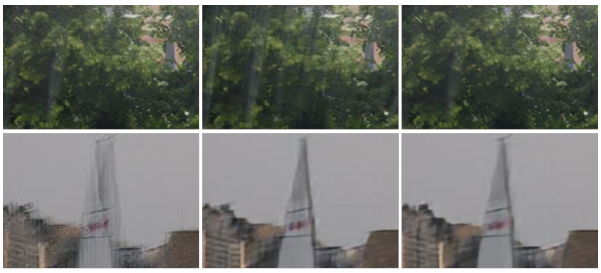

Figure 5. Qualitative results evaluated on the real rain (top) and real blur (bottom) for Ours (well on both), Chen [12] (well on one) and AirNet [26] (well on the other) trained on synthetic data.

clusters based on degradation types. Low discriminative power of the CE in AirNet seems to be responsible for low performance in Rain-Snow-Haze, while our proposed DC with high discriminative power contributed to robust performance in both Rain-Blur-Noise with different degradation models and Rain-Snow-Haze with similar models.

6. Discussion

Furthermore, we evaluated our method trained with synthetic data for real rain [58] and real blur [24] and the results in the Figure 5, yielding excellent performance in both cases over prior arts such as Chen [12] and AirNet [26]. Even though our current work achieved excellent performance on real rain and blur datasets qualitatively, there might be a domain gap between synthetic and real degraded images, which can be exciting and important future challenges.

7. Conclusion

We proposed ADMS, all-in-one image restoration method for unknown multiple degradations with ADS using our FAIG-SD and DC. Our proposed method with explicit parameter disentanglement for multiple degradations outperform state-of-the-art all-in-one image restoration methods on both Rain-Snow-Haze and Rain-Noise-Blur.

Acknowledgments This work was supported by the National Research Foundation of Korea(NRF) grants funded by the Korea government(MSIT) (NRF-2022R1A4A1030579), Basic Science Research Program through the NRF funded by the Ministry of Education(NRF-2017R1D1A1B05035810) and a grant of the Korea Health Technology R&D Project through the Korea Health Industry Development Institute (KHIDI), funded by the Ministry of Health & Welfare, Republic of Korea (grant number : HI18C0316). Also, the authors acknowledged the financial supports from BK21 FOUR program of the Education and Research Program for Future ICT Pioneers, Seoul National University.

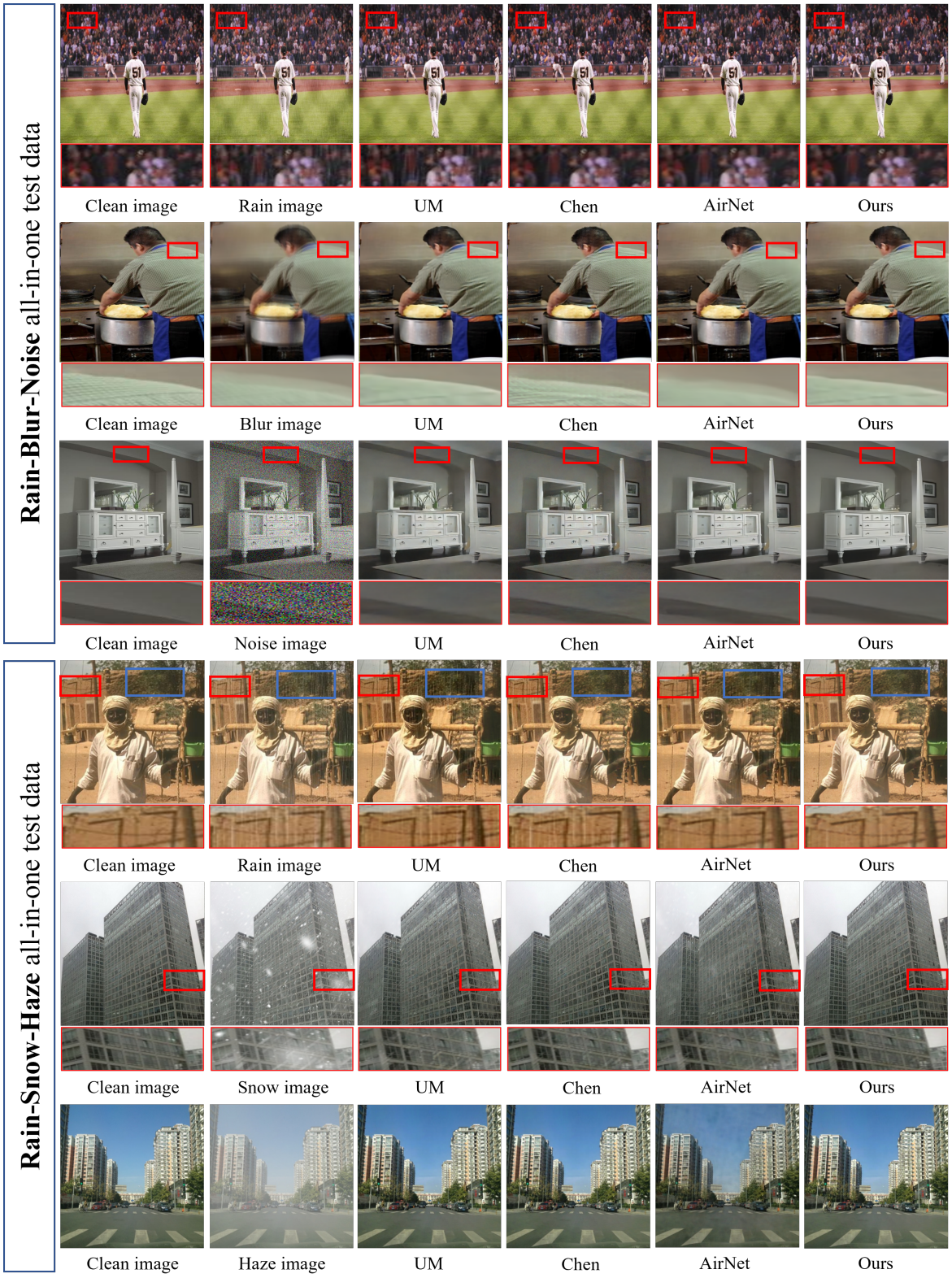

Figure 6. Qualitative results evaluated on the Rain-Blur-Noise and Rain-Snow-Haze test datasets for our proposed method, generic unified model(UM), Chen [12] and AirNet [26]. Our proposed method yielded visually excellent results for the multiple degradations.

References

[1] Cosmin Ancuti, Codruta Orniana Ancuti, Tom Haber, and Philippe Bekaert. Enhancing underwater images and videos by fusion. In *CVPR*, 2012. 3

[2] Joshua Batson and Loic Royer. Noise2self: Blind denoising by self-supervision. In *ICML*, 2019. 1

[3] Mariusz Bojarski, Davide Del Testa, Daniel Dworakowski, Bernhard Firner, Beat Flepp, Prasoon Goyal, Lawrence D Jackel, Mathew Monfort, Urs Muller, Jiakai Zhang, et al. End to end learning for self-driving cars. *NIPS Deep Learning Symposium*, 2016. 1

[4] Tim Brooks, Ben Mildenhall, Tianfan Xue, Jiawen Chen, Dillon Sharlet, and Jonathan T Barron. Unprocessing images for learned raw denoising. In *CVPR*, 2019. 1

[5] Chenghao Chen and Hao Li. Robust representation learning with feedback for single image deraining. In *CVPR*, 2021. 1

[6] Hanting Chen, Yunhe Wang, Tianyu Guo, Chang Xu, Yiping Deng, Zhenhua Liu, Siwei Ma, Chunjing Xu, Chao Xu, and Wen Gao. Pre-trained image processing transformer. In *CVPR*, 2021. 3

[7] Liangyu Chen, Xiaojie Chu, Xiangyu Zhang, and Jian Sun. Simple baselines for image restoration. *ECCV*, 2022. 1, 3, 5

[8] Liangyu Chen, Xin Lu, Jie Zhang, Xiaojie Chu, and Chengpeng Chen. Hinet: Half instance normalization network for image restoration. In *CVPR*, 2021. 1

[9] Wei-Ting Chen, Hao-Yu Fang, Jian-Jiun Ding, and Sy-Yen Kuo. Pmhld: Patch map-based hybrid learning dehazenet for single image haze removal. *IEEE TIP*, 2020. 1

[10] Wei-Ting Chen, Hao-Yu Fang, Jian-Jiun Ding, Cheng-Che Tsai, and Sy-Yen Kuo. Jstasr: Joint size and transparency-aware snow removal algorithm based on modified partial convolution and veiling effect removal. In *ECCV*, 2020. 3

[11] Wei-Ting Chen, Hao-Yu Fang, Cheng-Lin Hsieh, Cheng-Che Tsai, I Chen, Jian-Jiun Ding, Sy-Yen Kuo, et al. All snow removed: Single image desnowing algorithm using hierarchical dual-tree complex wavelet representation and contradict channel loss. In *ICCV*, 2021. 1, 3, 5

[12] Wei-Ting Chen, Zhi-Kai Huang, Cheng-Che Tsai, Hao-Hsiang Yang, Jian-Jiun Ding, and Sy-Yen Kuo. Learning multiple adverse weather removal via two-stage knowledge learning and multi-contrastive regularization: Toward a unified model. In *CVPR*, 2022. 1, 3, 5, 6, 7, 8

[13] X Chu, L Chen, C Chen, and X Lu. Improving image restoration by revisiting global information aggregation. *ECCV*, 2022. 1

[14] Chao Dong, Chen Change Loy, Kaiming He, and Xiaoou Tang. Image super-resolution using deep convolutional networks. *IEEE TPAMI*, 2015. 4

[15] Hang Dong, Jinshan Pan, Lei Xiang, Zhe Hu, Xinyi Zhang, Fei Wang, and Ming-Hsuan Yang. Multi-scale boosted dehazing network with dense feature fusion. In *CVPR*, 2020. 5

[16] Xueyang Fu, Jiabin Huang, Delu Zeng, Yue Huang, Xinghao Ding, and John Paisley. Removing rain from single images via a deep detail network. In *CVPR*, 2017. 1, 5

[17] Kaiming He, Xiangyu Zhang, Shaoqing Ren, and Jian Sun. Deep residual learning for image recognition. In *CVPR*, 2016. 1

[18] Ming Hong, Yuan Xie, Cuihua Li, and Yanyun Qu. Distilling image dehazing with heterogeneous task imitation. In *CVPR*, 2020. 1

[19] Xiaobin Hu, Wenqi Ren, Kaicheng Yu, Kaihao Zhang, Xiaochun Cao, Wei Liu, and Bjoern Menze. Pyramid architecture search for real-time image deblurring. In *ICCV*, 2021. 1

[20] Tao Huang, Songjiang Li, Xu Jia, Huchuan Lu, and Jianzhuang Liu. Neighbor2neighbor: Self-supervised denoising from single noisy images. In *CVPR*, 2021. 1

[21] Xiangtao Kong, Hengyuan Zhao, Yu Qiao, and Chao Dong. Classsr: A general framework to accelerate super-resolution networks by data characteristic. In *CVPR*, 2021. 3

[22] Alex Krizhevsky, Ilya Sutskever, and Geoffrey E Hinton. Imagenet classification with deep convolutional neural networks. *NIPS*, 2012. 1

[23] Orest Kupyn, Volodymyr Budzan, Mykola Mykhailych, Dmytro Mishkin, and Jiří Matas. Deblurgan: Blind motion deblurring using conditional adversarial networks. In *CVPR*, 2018. 1

[24] Wei-Sheng Lai, Jia-Bin Huang, Zhe Hu, Narendra Ahuja, and Ming-Hsuan Yang. A comparative study for single image blind deblurring. In *CVPR*, 2016. 1, 7

[25] Jaakko Lehtinen, Jacob Munkberg, Jon Hasselgren, Samuli Laine, Tero Karras, Miika Aittala, and Timo Aila. Noise2noise: Learning image restoration without clean data. *ICML*, 2018. 1, 5

[26] Boyun Li, Xiao Liu, Peng Hu, Zhongqin Wu, Jiancheng Lv, and Xi Peng. All-in-one image restoration for unknown corruption. In *CVPR*, 2022. 1, 2, 3, 5, 6, 7, 8

[27] Boyi Li, Xiulian Peng, Zhangyang Wang, Jizheng Xu, and Dan Feng. Aod-net: All-in-one dehazing network. In *ICCV*, 2017. 1

[28] Boyi Li, Wenqi Ren, Dengpan Fu, Dacheng Tao, Dan Feng, Wenjun Zeng, and Zhangyang Wang. Benchmarking single-image dehazing and beyond. *IEEE TIP*, 2018. 5

[29] Ruoteng Li, Robby T Tan, and Loong-Fah Cheong. All in one bad weather removal using architectural search. In *CVPR*, 2020. 1, 3, 6

[30] Xia Li, Jianlong Wu, Zhouchen Lin, Hong Liu, and Hongbin Zha. Recurrent squeeze-and-excitation context aggregation net for single image deraining. In *ECCV*, 2018. 1

[31] Zhi Li, Juan Zhang, Zhijun Fang, Bo Huang, Xiaoyan Jiang, Yongbin Gao, and Jenq-Neng Hwang. Single image snow removal via composition generative adversarial networks. *IEEE Access*, 2019. 1

[32] Xiaohong Liu, Yongrui Ma, Zhihao Shi, and Jun Chen. Griddehazenet: Attention-based multi-scale network for image dehazing. In *ICCV*, 2019. 1

[33] Yun-Fu Liu, Da-Wei Jaw, Shih-Chia Huang, and Jenq-Neng Hwang. Desnownet: Context-aware deep network for snow removal. *IEEE TIP*, 2018. 1

[34] Chenxu Luo, Xiaodong Yang, and Alan Yuille. Self-supervised pillar motion learning for autonomous driving. In *CVPR*, 2021. 1

[35] Chong Mou, Qian Wang, and Jian Zhang. Deep generalized unfolding networks for image restoration. In *CVPR*, 2022. 1, 3

[36] Seungjun Nah, Tae Hyun Kim, and Kyoung Mu Lee. Deep multi-scale convolutional neural network for dynamic scene deblurring. In *CVPR*, 2017. 1

[37] Srinivasa G Narasimhan and Shree K Nayar. Vision and the atmosphere. *IJCV*, 2002. 3

[38] Dongwon Park, Dong Un Kang, Jisoo Kim, and Se Young Chun. Multi-temporal recurrent neural networks for progressive non-uniform single image deblurring with incremental temporal training. In *ECCV*, 2020. 1

[39] Kuldeep Purohit, Maitreya Suin, AN Rajagopalan, and Vishnu Naresh Boddeti. Spatially-adaptive image restoration using distortion-guided networks. In *ICCV*, 2021. 1, 3

[40] Xu Qin, Zhilin Wang, Yuanchao Bai, Xiaodong Xie, and Huizhu Jia. Ffa-net: Feature fusion attention network for single image dehazing. In *AAAI*, 2020. 1

[41] Joseph Redmon, Santosh Divvala, Ross Girshick, and Ali Farhadi. You only look once: Unified, real-time object detection. In *CVPR*, 2016. 1

[42] Shaoqing Ren, Kaiming He, Ross Girshick, and Jian Sun. Faster r-cnn: Towards real-time object detection with region proposal networks. *NIPS*, 2015. 1

[43] Jaesung Rim, Geonung Kim, Jungeon Kim, Junyong Lee, Seungyong Lee, and Sunghyun Cho. Realistic blur synthesis for learning image deblurring. *ECCV*, 2022. 1, 5

[44] Jaesung Rim, Haeyun Lee, Jucheol Won, and Sunghyun Cho. Real-world blur dataset for learning and benchmarking deblurring algorithms. In *ECCV*, 2020. 5

[45] Yuanjie Shao, Lerenhan Li, Wenqi Ren, Changxin Gao, and Nong Sang. Domain adaptation for image dehazing. In *CVPR*, 2020. 1

[46] Shuochen Su, Mauricio Delbracio, Jue Wang, Guillermo Sapiro, Wolfgang Heidrich, and Oliver Wang. Deep video deblurring for hand-held cameras. In *CVPR*, 2017. 1

[47] Mukund Sundararajan, Ankur Taly, and Qiqi Yan. Gradients of counterfactuals. *arXiv preprint arXiv:1611.02639*, 2016. 3

[48] Mukund Sundararajan, Ankur Taly, and Qiqi Yan. Axiomatic attribution for deep networks. In *ICML*, 2017. 3

[49] Yuandong Tian and Srinivasa G Narasimhan. Seeing through water: Image restoration using model-based tracking. In *ICCV*, 2009. 3

[50] Zhengzhong Tu, Hossein Talebi, Han Zhang, Feng Yang, Peyman Milanfar, Alan Bovik, and Yinxiao Li. Maxim: Multi-axis mlp for image processing. In *CVPR*, 2022. 1, 3

[51] Guoqing Wang, Changming Sun, and Arcot Sowmya. Erl-net: Entangled representation learning for single image deraining. In *ICCV*, 2019. 1

[52] Hong Wang, Qi Xie, Qian Zhao, and Deyu Meng. A model-driven deep neural network for single image rain removal. In *CVPR*, 2020. 1

[53] Yinglong Wang, Shuaicheng Liu, Chen Chen, and Bing Zeng. A hierarchical approach for rain or snow removing in a single color image. *IEEE TIP*, 2017. 1

[54] Zhendong Wang, Xiaodong Cun, Jianmin Bao, Wengang Zhou, Jianzhuang Liu, and Houqiang Li. Uformer: A general u-shaped transformer for image restoration. In *CVPR*, 2022. 1, 3

[55] Jay Whang, Mauricio Delbracio, Hossein Talebi, Chitwan Saharia, Alexandros G Dimakis, and Peyman Milanfar. Deblurring via stochastic refinement. In *CVPR*, 2022. 1

[56] Haiyan Wu, Yanyun Qu, Shaohui Lin, Jian Zhou, Ruizhi Qiao, Zhizhong Zhang, Yuan Xie, and Lizhuang Ma. Contrastive learning for compact single image dehazing. In *CVPR*, 2021. 1

[57] Liangbin Xie, Xintao Wang, Chao Dong, Zhongang Qi, and Ying Shan. Finding discriminative filters for specific degradations in blind super-resolution. *NeurIPS*, 2021. 2, 3, 4

[58] Wenhan Yang, Robby T Tan, Jiashi Feng, Jiaying Liu, Zongming Guo, and Shuicheng Yan. Deep joint rain detection and removal from a single image. In *CVPR*, 2017. 3, 7

[59] Wenhan Yang, Robby T Tan, Shiqi Wang, Yuming Fang, and Jiaying Liu. Single image deraining: From model-based to data-driven and beyond. *IEEE TPAMI*, 2020. 1

[60] Rajeev Yasarla, Vishwanath A Sindagi, and Vishal M Patel. Syn2real transfer learning for image deraining using gaussian processes. In *CVPR*, 2020. 1

[61] Syed Waqas Zamir, Aditya Arora, Salman Khan, Munawar Hayat, Fahad Shahbaz Khan, and Ming-Hsuan Yang. Restormer: Efficient transformer for high-resolution image restoration. In *CVPR*, 2022. 1, 3

[62] Syed Waqas Zamir, Aditya Arora, Salman Khan, Munawar Hayat, Fahad Shahbaz Khan, Ming-Hsuan Yang, and Ling Shao. Multi-stage progressive image restoration. In *CVPR*, 2021. 1, 3

[63] He Zhang and Vishal M Patel. Densely connected pyramid dehazing network. In *CVPR*, 2018. 1

[64] He Zhang and Vishal M Patel. Density-aware single image de-raining using a multi-stream dense network. In *CVPR*, 2018. 5

[65] Kai Zhang, Wangmeng Zuo, Yunjin Chen, Deyu Meng, and Lei Zhang. Beyond a gaussian denoiser: Residual learning of deep cnn for image denoising. *IEEE TIP*, 2017. 1

[66] Zhuoran Zheng, Wenqi Ren, Xiaochun Cao, Xiaobin Hu, Tao Wang, Fenglong Song, and Xiuyi Jia. Ultra-high-definition image dehazing via multi-guided bilateral learning. In *CVPR*, 2021. 1

[67] Magauiya Zhussip, Shakarim Soltanayev, and Se Young Chun. Extending stein's unbiased risk estimator to train deep denoisers with correlated pairs of noisy images. *NeurIPS*, 2019. 1, 5

[68] Magauiya Zhussip, Shakarim Soltanayev, and Se Young Chun. Training deep learning based image denoisers from undersampled measurements without ground truth and without image prior. In *CVPR*, 2019. 1, 5